Fayyaz Ahmad, Mubbashar Nazeer\*, Mubashara Saeed, Adila Saleem and Waqas Ali

# Heat and Mass Transfer of Temperature-Dependent Viscosity Models in a Pipe: Effects of Thermal Radiation and Heat Generation

https://doi.org/10.1515/zna-2019-0332 Received November 10, 2019; accepted December 30, 2019; previously published online February 7, 2020

**Abstract:** In this paper, a study of the flow of Eyring-Powell (EP) fluid in an infinite circular long pipe under the consideration of heat generation and thermal radiation is considered. It is assumed that the viscosity of the fluid is an exponential function of the temperature of the fluid. The flow of fluid depends on many variables, such as the physical property of each phase and shape of solid particles. To convert the given governing equations into dimensionless form, the dimensionless quantities have been used and the resultant boundary value problem is solved for the calculation of velocity and temperature fields. The analytical solutions of velocity and temperature are calculated with the help of the perturbation method. The effects of the fluidic parameters on velocity and temperature are discussed in detail. Finite difference method is employed to find the numerical solutions and compared with the analytical solution. The magnitude error in velocity and temperature is obtained in each case of the viscosity model and plotted against the radius of the pipe. Graphs are plotted to describe the influence of various parameter EP parameters, heat generation parameter and thermal radiation parameters against velocity and temperature profiles. The fluid temperature has decreasing and increasing trends with respect to radiation and heat generations parameters, respectively.

**Keywords:** Eyring-Powell Fluid; Finite Difference Method; Heat Generation; Perturbation Technique; Thermal Radiations.

Fayyaz Ahmad: Department of Applied Sciences, National Textile University, Faisalabad 37610, Pakistan, E-mail: fayyaz.ahmad@ntu.edu.pk

Mubashara Saeed and Adila Saleem: Department of Mathematics, Riphah International University, Faisalabad Campus, Faisalabad 38000, Pakistan, E-mail: mubasharasaeed0302@gmail.com (M. Saeed); adilasaleem527@gmail.com (A. Saleem)

**Waqas Ali:** Chair of Production Technology, Faculty of Engineering Technology, University of Twente, Enschede, The Netherlands, E-mail: w.ali@utwente.nl

### 1 Introduction

The study of non-Newtonian fluids has increased due to a substantial variety of engineering, industrial and commercial manufacturing applications. The study of Newtonian fluids is easy as compared to non-Newtonian fluids due to simple developed equations which can be handled numerically or analytically. The reason is that of a linear relationship between the rate of stress and strain in the case of Newtonian fluid, but this relation is not any more linear for non-Newtonian fluids. Various authors showed the applications of non-Newtonian fluids in their studies. Some significant examples of non-Newtonian fluids are cream, plastic melts, soap slurries, wet beach sand, mayonnaise, paper pulp, etc. [1]. Navier-Stokes equation is used to describe the flow behaviour of Newtonian fluid but there is no single equation to describe the flow behaviour of the non-Newtonian fluids with all the properties. Due to this reason, various empirical and semi-empirical non-Newtonian equations or models have been presented and used.

Ali et al. [2] studied an Eyring-Powell (EP) fluid under the effects of temperature-dependent viscosity cases in a pipe. They first convert their dimensional forms of momentum and energy equations with boundary conditions into non-dimensional form, and then discuss Reynolds and Vogel models for both momentum and energy equations. In their research work, they solved their equations with the help of both perturbation and numerical methods that match well. The flow of magnetohydrodynamics (MHD) EP nanofluid over an inclined surface is analysed by Khan et al. [3]. During their study, they assumed that the flow of fluid is incompressible and the fluid viscosity is varying exponentially. They expressed their results in the form of velocity and temperature profiles along with different parameters by plotting graphs and also in tabular form. Ellahi [4] examined the study of non-Newtonian nanofluid in the pipe and depicted the effects of magnetic and temperature-dependent viscosity. Akinshilo and Olaye [5] also analysed the flow of EP fluid in a pipe. They discussed the internal heat flow and temperature-dependent viscosity in their work. They solved the non-linear ordinary equation by using perturbation technique and examined the effect of fluidic parameters on velocity and temperature profiles. Akinbowale [6] studied the non-Newtonian

<sup>\*</sup>Corresponding author: Mubbashar Nazeer, Department of Mathematics, Riphah International University, Faisalabad Campus, Faisalabad 38000, Pakistan, E-mail: mubbashariiui@gmail.com. https://orcid.org/0000-0002-3932-6214

flow of third-grade fluid in the horizontal channel. He solved an ordinary differential equation by using Adomian decomposition method and discussed the Vogel model for temperature-dependent viscosity and concluded that velocity distribution increases by decreasing the porosity parameter. Ellahi and Riaz [7] captured the magnetic effects in the flow of third-grade fluid in a pipe by taking variable viscosity. To calculate the analytical solution, the homotopy analysis method (HAM) was used. Aksoy and Pakdemirli [8] considered the non-Newtonian fluid with a porous medium between two parallel plates. They calculated the solutions of the non-linear differential equations by employing the perturbation technique. Three viscosity dependent cases were discussed i.e., (a) constant viscosity case; (b) Reynolds model; and (c) Vogel's model. The validity range of the solution was also provided. Ellahi et al. [9] examined the third-grade fluid between the concentric cylinders and checked the effect of slip over this fluid. They discussed two cases, in the first one the outer cylinder is stationary and inner cylinder move and the second one the outer cylinder is moving and the inner cylinder is at rest position. They calculate the solutions for both conditions (with and without slip parameter). The flow of nonisothermal Poiseuille fluid was also examined by Faroog et al. [10]. They considered the fluid is flowing between two heated parallel inclined plates using coupled stress fluid which was incompressible. Perturbation techniques were used to calculate analytical solutions. In their paper, they discussed the Reynold's model and obtained the expressions for temperature, velocity, dynamic pressure, shear stress and volume flow rate. Alharbi et al. [11] evaluated the effects of entropy generation in MHD EP fluid. They assumed that the flow is flowing over an oscillating porous stretching sheet and further assumed that the flow is unsteady. They analysed the behaviour of the heat source and thermal radiation in their study. They captured the effects of pertinent parameters on entropy generation rate, temperature, and velocity fields. They solved the governing equation by using HAM. The radiative effect on three-dimensional MHD flow of an EP fluid was described by Hayat et al. [12]. They calculated the series solution by non-linear analysis and also calculate the exact solution of the problem. Yurusoy [13] presented the heat transfer effects of third-grade fluid between two concentric cylinders. During his study, he considered that the fluid temperature is lower than the pipe temperature. He calculated the solution by using perturbation technique and discussed Reynolds model. Hayat et al. [14] explored the effect of porous medium of third-grade fluid. They solved the governing momentum and energy equations by employing HAM. They analysed the shear stress and velocity field at

the plate. Massoudi and Christie [15] analysed the viscous dissipation and variable viscosity effects of third-grade fluid in a pipe and considered that the temperature of the fluid is lower than the temperature of the pipe. Huang [16] studied the heat generation effect of non-Newtonian fluid over a vertical permeable cone in a porous medium. The author used the Keller box method to find a solution of his problem and discussed the physical aspects of the problem. Analysis of EP nanofluid is selected by Hayat et al. [17]. They captured the effect of MHD flow over the nonlinear stretching sheet and discussed the results for concentration and temperature profiles. Hayat and Nadeem [18] studied the three-dimensional flow of EP fluid and discussed the heat flux and mass quantities. They discussed the behaviour of temperature and Cattaneo-Christov heat flux theory.

From the above-cited studies, it is noted that there is no study available in literature to capture the effects of radiative heat flux and heat generation on EP fluid in a circular long pipe under various models of the viscosities. The considered fluid model (EP) is much complex and is advantageous over a Power-law model due to two aspects. The first one is that this model is not driven from an empirical relation like a Power-law model. The second one is, this fluid model can be reduced into a Newtonian fluid model for the low and high shear rates. Therefore, the objective of our investigation is to obtain the numerical and perturbation solutions of the one-dimensional flow of an EP fluid in a pipe under the combined effects of radiative and heat absorption. As various engineering processes only happen at moderate temperature, so the consideration of radiative heat flux cannot be ignored in these kind of processes namely space vehicles, gas turbines, propulsion devices, and nuclear plants [19, 20]. Futher, the study of heat generation (or absorption) in moving fluid is useful in the problems of chemical reaction. The flows in the porous media have numerious applications like, oil reservoir and geothermal [21, 22]. The absolute error in velocity and temperature will be presented. Three famous models will discuss which are listed below.

- (a) Constant viscosity model
- (b) Reynolds model
- (c) Vogel's model

The numerical solution for all above-mentioned viscosity models will be obtained by the finite-difference method in our study. The effects of various physical parameters on viscosity and temperature profiles will be highlighted together with the validity of the perturbation solution. The current study can be useful to increase the heat transfer processes in energy conservation, medical

process, fuel cells and micro-mixing. The applications of this problem are also beneficial in heat exchangers, film flow, catalytic reactors, paper production and polymer solutions. This study will be helpful in future to investigate the behaviour of velocity and temperature fields against pertinent prameters, whenever preliminary data of EP model is given.

### Formulation of the Problem

Let us consider the one-dimensional, steady-state flow of non-Newtonian fluid in a pipe with the account of effects of radiation and heat generation. It is assuming that the flow is flowing due to applied pressure gradient and the viscosity is a function of temperature. The systematic flow behaviour is shown in Figure 1.

The velocity and temperature fields for the present problem are defined by

$$\mathbf{V} = (0, 0, w(r)) \tag{1}$$

$$\theta = \theta(r),$$
 (2)

The Cauchy stress tensor T[23, 24] is

$$\mathbf{T} = -p\mathbf{I} + \mathbf{S},\tag{3}$$

where p is the pressure, **I** is the identity element. Now for the current situation, the extra stress tensor S is defined as

$$\mathbf{S} = \left(\mu + \frac{1}{k^2} \frac{\sinh^{-1}(k_3 \theta)}{\theta}\right) \mathbf{A}_1,\tag{4}$$

where

$$\vartheta = \sqrt{\frac{1}{2} \operatorname{tra}(\mathbf{A}_1)^2},\tag{5}$$

and

$$\mathbf{A}_1 = \operatorname{grad} \mathbf{V} + \operatorname{grad}(\mathbf{V})^T, \tag{6}$$

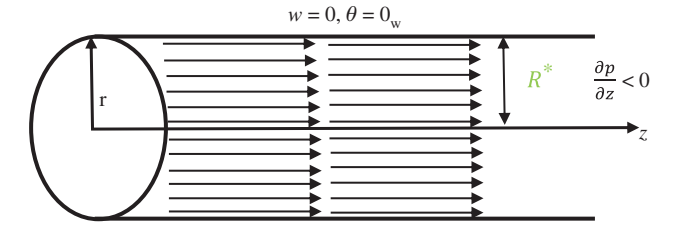


Figure 1: Geometry of the flow problem.

$$\operatorname{grad} \mathbf{V} = \mathbf{L} = \begin{pmatrix} \frac{\mathrm{d}u}{\mathrm{d}r} & \frac{1}{r} \frac{\mathrm{d}u}{\mathrm{d}\theta} - \frac{v}{r} & \frac{\mathrm{d}u}{\mathrm{d}z} \\ \frac{\mathrm{d}v}{\mathrm{d}r} & \frac{1}{r} \frac{\mathrm{d}v}{\mathrm{d}\theta} + \frac{u}{r} & \frac{\mathrm{d}v}{\mathrm{d}z} \\ \frac{\mathrm{d}w}{\mathrm{d}r} & \frac{1}{r} \frac{\mathrm{d}w}{\mathrm{d}\theta} & \frac{\mathrm{d}w}{\mathrm{d}z} \end{pmatrix}, \tag{7}$$

As  $\mathbf{V} = [u, v, w]$  and in our case  $\mathbf{V} = [0, 0, w(r)]$ , so in this case, we have

$$\mathbf{L} = \begin{pmatrix} 0 & 0 & 0 \\ 0 & 0 & 0 \\ \frac{dw}{dr} & 0 & 0 \end{pmatrix}, \quad \mathbf{L}^T = \begin{pmatrix} 0 & 0 & \frac{dw}{dr} \\ 0 & 0 & 0 \\ 0 & 0 & 0 \end{pmatrix}$$
(8)

$$\mathbf{A}_{1} = \begin{pmatrix} 0 & 0 & \frac{\mathrm{d}w}{\mathrm{d}r} \\ 0 & 0 & 0 \\ \frac{\mathrm{d}w}{\mathrm{d}r} & 0 & 0 \end{pmatrix}, \quad (\mathbf{A}_{1})^{2} = \begin{pmatrix} 0 & 0 & \left(\frac{\mathrm{d}w}{\mathrm{d}r}\right)^{2} \\ 0 & 0 & 0 \\ \left(\frac{\mathrm{d}w}{\mathrm{d}r}\right)^{2} & 0 & 0 \end{pmatrix},$$
(9)

$$\operatorname{tra}\left(\left(\mathbf{A}_{1}\right)^{2}\right)=2\left(\frac{\mathrm{d}w}{\mathrm{d}r}\right)^{2},\tag{10}$$

$$\theta = \sqrt{\frac{1}{2} \operatorname{tra}(\mathbf{A}_1)^2},\tag{11}$$

with the help of (10), we get

$$\theta = \frac{\mathrm{d}w}{\mathrm{d}r}.\tag{12}$$

Putting these values in (4), (4) takes the following form:

$$\mathbf{S} = \left(\mu + \frac{1}{k^2} \left( \left(\frac{\mathrm{d}w}{\mathrm{d}r}\right) \frac{k_3 - \frac{1}{6}k_3^3 \left(\frac{\mathrm{d}w}{\mathrm{d}r}\right)^2}{\left(\frac{\mathrm{d}w}{\mathrm{d}r}\right)} \right) \right) \mathbf{A}_1, \quad (13)$$

$$\mathbf{S} = \left(\mu + \frac{k_3}{k_2} - \frac{k_3^3}{k_2} \frac{1}{6} \left(\frac{\mathrm{d}w}{\mathrm{d}r}\right)^2\right) \mathbf{A}_1,\tag{14}$$

Using  $X = \frac{k_3}{k_3}$ ,  $Y = \frac{k_3^3}{k_2}$  in the above (14) becomes

$$\mathbf{S} = \left(\mu + X - \frac{Y}{6} \left(\frac{\mathrm{d}w}{\mathrm{d}r}\right)^2\right) \mathbf{A}_1, Y \ll 1 \tag{15}$$

Now by substituting the value of  $A_1$  in (15), we get

$$\mathbf{S} = \left(\mu + X - \frac{Y}{6} \left(\frac{dw}{dr}\right)^{2}\right) \begin{pmatrix} 0 & 0 & \frac{dw}{dr} \\ 0 & 0 & 0 \\ \frac{dw}{dr} & 0 & 0 \end{pmatrix}, \quad (16)$$

where S is defined as

$$\mathbf{S} = \begin{pmatrix} s_{rr} & s_{r\theta} & s_{rz} \\ s_{\theta r} & s_{\theta \theta} & s_{\theta z} \\ s_{zr} & s_{z\theta} & s_{zz} \end{pmatrix}, \tag{17}$$

Now using the value of S in (16)

$$\begin{pmatrix} s_{rr} & s_{r\theta} & s_{rz} \\ s_{\theta r} & s_{\theta \theta} & s_{\theta z} \\ s_{zr} & s_{z\theta} & s_{zz} \end{pmatrix}$$
 along z-direction only (one dimensional) so we can simple derivative instead of partial derivative sym 
$$= \begin{pmatrix} 0 & 0 & \left(\mu + X - \frac{Y}{6} \left(\frac{\mathrm{d}w}{\mathrm{d}r}\right)^2\right) \frac{\mathrm{d}w}{\mathrm{d}r} \\ 0 & 0 & 0 \\ \left(\mu + X - \frac{Y}{6} \left(\frac{\mathrm{d}w}{\mathrm{d}r}\right)^2\right) \frac{\mathrm{d}w}{\mathrm{d}r} & 0 \end{pmatrix}, \qquad \mu \frac{\mathrm{d}^2 w}{\mathrm{d}r^2} + \frac{\mu}{r} \frac{\mathrm{d}w}{\mathrm{d}r} + \frac{\mathrm{d}\mu}{\mathrm{d}r} \frac{\mathrm{d}w}{\mathrm{d}r} + X \left(\frac{1}{r} \frac{\mathrm{d}w}{\mathrm{d}r} + \frac{\mathrm{d}^2 w}{\mathrm{d}r^2}\right) \\ - \frac{Y}{6} \left(\frac{\mathrm{d}w}{\mathrm{d}r}\right)^2 \left(3r \frac{\mathrm{d}^2 w}{\mathrm{d}r^2} + \frac{\mathrm{d}w}{\mathrm{d}r}\right) = c_1,$$

From the above (18), only two components of extra stress are left which are:

$$s_{rz} = s_{zr} = \left(\mu + X - \frac{Y}{6} \left(\frac{\mathrm{d}w}{\mathrm{d}r}\right)^2\right) \left(\frac{\mathrm{d}w}{\mathrm{d}r}\right), \quad (19)$$

The general form of the equation of motion in cylindrical coordinates system is:

$$\rho \left( \frac{\mathrm{d}}{\mathrm{d}t} + u \frac{\mathrm{d}}{\mathrm{d}r} + \frac{v}{r} \frac{\mathrm{d}}{\mathrm{d}\theta} + w \frac{\mathrm{d}}{\mathrm{d}z} \right) u$$

$$= -\frac{\partial p}{\partial r} + \frac{1}{r} \frac{\partial}{\partial r} (r s_{rr}) + \frac{\partial s_{rr}}{\partial z} - \frac{1}{r} s_{\theta\theta} + \rho g_u, \quad (20)$$

$$\rho \left( \frac{\mathrm{d}}{\mathrm{d}t} + u \frac{\mathrm{d}}{\mathrm{d}r} + \frac{v}{r} \frac{\mathrm{d}}{\mathrm{d}\theta} + \frac{uw}{r} + w \frac{\mathrm{d}}{\mathrm{d}z} \right) v$$

$$= -\frac{1}{r} \frac{\partial p}{\partial \theta} + \frac{1}{r^2} \frac{\partial}{\partial r} \left( r^2 s_{r\theta} \right) + \frac{1}{r} \frac{\partial s_{\theta\theta}}{\partial \theta} + \frac{\partial s_{z\theta}}{\partial z}$$

$$+ \frac{1}{r} (s_{\theta r} - s_{r\theta}) + \rho g_v, \tag{21}$$

$$\rho \left( \frac{\mathrm{d}}{\mathrm{d}t} + u \frac{\mathrm{d}}{\mathrm{d}r} + \frac{v}{r} \frac{\mathrm{d}}{\mathrm{d}\theta} + w \frac{\mathrm{d}}{\mathrm{d}z} \right) w$$

$$= -\frac{\partial p}{\partial z} + \frac{1}{r} \frac{\partial}{\partial r} (r s_{rz}) + \frac{1}{r} \frac{\partial s_{\theta z}}{\partial \theta} + \frac{\partial s_{zz}}{\partial z} + \rho g_w, \quad (22)$$

Due to steady-state flow, we have

$$\rho \left( u \frac{\mathrm{d}}{\mathrm{d}r} + \frac{v}{r} \frac{\mathrm{d}}{\mathrm{d}\theta} + w \frac{\mathrm{d}}{\mathrm{d}z} \right) u = -\frac{\partial p}{\partial r}, \tag{23}$$

$$\rho\left(u\frac{\mathrm{d}}{\mathrm{d}r} + \frac{v}{r}\frac{\mathrm{d}}{\mathrm{d}\theta} + \frac{uw}{r} + w\frac{\mathrm{d}}{\mathrm{d}z}\right)v = -\frac{1}{r}\frac{\partial p}{\partial \theta},\tag{24}$$

$$\rho\left(u\frac{\mathrm{d}}{\mathrm{d}r} + \frac{v}{r}\frac{\mathrm{d}}{\mathrm{d}\theta} + w\frac{\mathrm{d}}{\mathrm{d}z}\right)w = -\frac{\partial p}{\partial z} + \frac{1}{r}\frac{\partial}{\partial r}(rs_{rz}), \quad (25)$$

As the velocity components u = 0 and v = 0 so, lefthand side of general equations will vanish and only righthand side will survive which is given by:

$$\frac{\partial p}{\partial r} = 0, \Rightarrow p \neq p(r)$$
 (26)

$$\frac{1}{r}\frac{\partial p}{\partial \theta} = 0, \Rightarrow p \neq p(\theta)$$
 (27)

$$\frac{1}{r}\frac{\mathrm{d}}{\mathrm{d}r}\left(r\mu\frac{\mathrm{d}w}{\mathrm{d}r} + Xr\frac{\mathrm{d}w}{\mathrm{d}r} - \frac{Yr}{6}\left(\frac{\mathrm{d}w}{\mathrm{d}r}\right)^{3}\right) = \frac{\partial p}{\partial z},\qquad(28)$$

As, in the current investigation, the flow is flowing along z-direction only (one dimensional) so we can use the simple derivative instead of partial derivative symbols.

$$\mu \frac{\mathrm{d}^2 w}{\mathrm{d}r^2} + \frac{\mu}{r} \frac{\mathrm{d}w}{\mathrm{d}r} + \frac{\mathrm{d}\mu}{\mathrm{d}r} \frac{\mathrm{d}w}{\mathrm{d}r} + X \left( \frac{1}{r} \frac{\mathrm{d}w}{\mathrm{d}r} + \frac{\mathrm{d}^2 w}{\mathrm{d}r^2} \right)$$
$$- \frac{Y}{6} \left( \frac{\mathrm{d}w}{\mathrm{d}r} \right)^2 \left( 3r \frac{\mathrm{d}^2 w}{\mathrm{d}r^2} + \frac{\mathrm{d}w}{\mathrm{d}r} \right) = c_1, \tag{29}$$

where  $\frac{\partial p}{\partial z} = c_1$ .

Now for the derivation of the heat equation, first the general form of the heat equation is considered

$$\rho c_{\rm p} \frac{\mathrm{d}\theta}{\mathrm{d}t} = \mathrm{tr}(S.L) - \mathrm{div}q + Q(\theta - \theta_{\rm w}) - \frac{\mathrm{d}H_{\rm R}}{\mathrm{d}r}, \quad (30)$$

$$\therefore \theta = \theta(r) \Rightarrow \frac{\mathrm{d}\theta}{\mathrm{d}t} = 0$$

$$0 = tr(\mathbf{S.L}) - div\mathbf{q}, \tag{31}$$

tra(**S.L**) = 
$$\left(\mu + X - \frac{Y}{6} \left(\frac{\mathrm{d}w}{\mathrm{d}r}\right)^2\right) \left(\frac{\mathrm{d}w}{\mathrm{d}r}\right)^2$$
, (32)

$$\operatorname{div}\mathbf{q} = -k\left(\frac{\mathrm{d}^2\theta}{\mathrm{d}r^2} + \frac{1}{r}\frac{\mathrm{d}\theta}{\mathrm{d}r}\right),\tag{33}$$

The radiative heat flux  $H_R$  [25, 26] for the current situation is defined by

$$H_{\rm R} = \frac{-4\sigma^*}{3kk^*} \frac{\mathrm{d}\theta^4}{\mathrm{d}r},\tag{34}$$

To obtain the values of  $\theta^4$ , we will expand  $\theta^4$  in the Taylor series expansion about  $\theta_w$  and overlooking upper order terms, yields

$$\theta^4 = \theta_w^4 + 4\theta_w^3(\theta - \theta_w),$$
 (35)

$$\frac{\mathrm{d}\theta^4}{\mathrm{d}r} = 4\theta_{\mathrm{W}}^3 \frac{\mathrm{d}\theta}{\mathrm{d}r},\tag{36}$$

Using the value of  $\theta^4$  into (34), we have

$$H_{\rm R} = \frac{-4\sigma^*}{3k^*} \cdot 4\theta_{\rm W}^3 \frac{{\rm d}\theta}{{\rm d}r}$$

Use (32), (33) and (34) into (31), we get

$$\mu \left(\frac{\mathrm{d}w}{\mathrm{d}r}\right)^{2} + X \left(\frac{\mathrm{d}w}{\mathrm{d}r}\right)^{2} - \frac{Y}{6} \left(\frac{\mathrm{d}w}{\mathrm{d}r}\right)^{4}$$

$$+ k \left(\frac{\mathrm{d}^{2}\theta}{\mathrm{d}r^{2}} + \frac{1}{r}\frac{\mathrm{d}\theta}{\mathrm{d}r}\right) + Q(\theta - \theta_{w})$$

$$+ \frac{16\sigma^{*}\theta_{w}^{3}}{3k^{*}}\frac{\mathrm{d}^{2}\theta}{\mathrm{d}r^{2}} = 0, \tag{37}$$

The boundary conditions for (29) and (37) are:

$$\left. \begin{array}{l} w=0, \\ \theta=\theta_{\rm W} \end{array} \right\} {\rm at} \ r=R^* \ {\rm and} \quad \left. \begin{array}{l} \frac{{\rm d}w}{{\rm d}r}=0, \\ \frac{{\rm d}\theta}{{\rm d}r}=0 \end{array} \right\} {\rm at} \ r=0 \quad (38)$$

Now introducing the dimensionless quantities

$$\hat{r} = \frac{r}{R^*}, \ \hat{w} = \frac{w}{w_0}, \ \hat{\theta} = \frac{\theta - \theta_w}{\theta_m - \theta_w}, \ \hat{\mu} = \frac{\mu}{\mu_0}$$
 (39)

The dimensionless equations are given by:

$$(1+R)\frac{d^{2}\widehat{\theta}}{d\widehat{r}^{2}} + \frac{1}{\widehat{r}}\frac{d\widehat{\theta}}{d\widehat{r}} + \delta\widehat{\theta}$$

$$+ \Gamma \left(\frac{d\widehat{w}}{d\widehat{r}}\right)^{2} \left[\widehat{\mu} + M - \Lambda \left(\frac{d\widehat{w}}{d\widehat{r}}\right)^{2}\right] = 0, \qquad (40)$$

$$\frac{d\hat{\mu}}{d\hat{r}}\frac{d\hat{w}}{d\hat{r}} + \frac{\hat{\mu}}{\hat{r}}\left(\frac{d\hat{w}}{d\hat{r}} + \hat{r}\frac{d^{2}\hat{w}}{d\hat{r}^{2}}\right) + \frac{M}{\hat{r}}\left(\frac{d\hat{w}}{d\hat{r}} + \hat{r}\frac{d^{2}\hat{w}}{d\hat{r}^{2}}\right) - \frac{\Lambda}{\hat{r}}\left(\frac{d\hat{w}}{d\hat{r}}\right)^{2}\left[\frac{d\hat{w}}{d\hat{r}} + 3\hat{r}\frac{d^{2}\hat{w}}{d\hat{r}^{2}}\right] = c,$$
(41)

$$\left. \begin{array}{l} \overset{\smile}{w} = 1, \\ \overset{\smile}{\theta} = 1 \end{array} \right\} \text{ at } r = 1 \text{ and } \left. \begin{array}{l} \frac{\mathrm{d} \overset{\smile}{w}}{\mathrm{d} \overset{\smile}{r}} = 0, \\ \frac{\mathrm{d} \overset{\smile}{\theta}}{\mathrm{d} \overset{\smile}{r}} = 0 \end{array} \right\} \text{ at } r = 0 \qquad (42)$$

where 
$$M = \frac{X}{\mu_0}$$
,  $c = \frac{c_1 R^{*2}}{\mu_0 w_0}$ ,  $\Gamma = \frac{\mu_0 w_0^2}{k(\theta_m - \theta_w)}$ ,  $\delta = \frac{QR^{*2}}{k}$ ,  $R = \frac{16\sigma^* \theta_w^3}{3k \, k^*}$  and  $\Lambda = \frac{Y_3^2 w_0^2}{6\mu_0 R^{*2}}$ 

The dimensionless equations of motion and energy based on viscosity models are discussed in the next one.

# 3 Viscosity Models

Based on the viscosity of the fluid, three different models are selected. In the first case, viscosity is chosen as a constant i.e., viscosity does not depend on temperature and in second and third cases, viscosity is a function of fluid temperature and these models are known as Reynolds and Vogel's models. In the last two models, viscosity is defined as an exponent form.

### - Constant Viscosity Model

For this case, we set  $\hat{\mu} = 1$ , therefore  $\frac{d\hat{\mu}}{d\hat{r}} = 0$ 

The new forms of the equation of motion and heat equation for the present case are:

$$\frac{1}{\hat{r}} \left( \frac{d\hat{w}}{d\hat{r}} + \hat{r} \frac{d^2 \hat{w}}{d\hat{r}^2} \right) + \frac{M}{\hat{r}} \left( \frac{d\hat{w}}{d\hat{r}} + \hat{r} \frac{d^2 \hat{w}}{d\hat{r}^2} \right) - \frac{\Lambda}{\hat{r}} \left( \frac{d\hat{w}}{d\hat{r}} \right)^2 \left[ \frac{d\hat{w}}{d\hat{r}} + 3\hat{r} \frac{d^2 \hat{w}}{d\hat{r}^2} \right] = c,$$
(43)

$$(1+R)\frac{\mathrm{d}^2\widehat{\theta}}{\mathrm{d}\widehat{r}^2} + \frac{1}{\widehat{r}}\frac{\mathrm{d}\widehat{\theta}}{\mathrm{d}\widehat{r}} + \delta\widehat{\theta}$$

$$+\Gamma\left(\frac{d\widehat{w}}{d\widehat{r}}\right)^{2}\left[1+M-\Lambda\left(\frac{d\widehat{w}}{d\widehat{r}}\right)^{2}\right]=0,$$
 (44)

$$\hat{w} = 0$$
 at  $\hat{r} = 1$ ,  $\hat{\theta} = 0$  at  $\hat{r} = 1$ , and

$$\frac{d\hat{w}}{d\hat{r}} = 0 \text{ at } \hat{r} = 0, \quad \frac{d\hat{\theta}}{d\hat{r}} = 0 \text{ at } \hat{r} = 0,$$
 (45)

To solve (43)–(45), let us assume to apply perturbation expansion on momentum and energy equation.

$$\hat{w} \cong \hat{w}_0 + \varepsilon \hat{w}_1, \quad \hat{\theta} \cong \hat{\theta}_0 + \varepsilon \hat{\theta}_1,$$

$$\Lambda \cong \varepsilon \sigma, \quad \delta = \varepsilon N_1, \tag{46}$$

where  $\epsilon$  is the perturbation parameter and (0 <  $\epsilon$   $\leq$  1). By separating each order of we have the following systems:

System of order ( $\epsilon^0$ ) for velocity profile:

$$\hat{r}\frac{\mathrm{d}^2\hat{w}_0}{\mathrm{d}\hat{r}^2} + \frac{\mathrm{d}\hat{w}_0}{\mathrm{d}\hat{r}} = \frac{c\hat{r}}{(1+M)},\tag{47}$$

$$\hat{w}_0 = 0$$
 at  $\hat{r} = 1$ ,  $\frac{d\hat{w}_0}{d\hat{r}} = 0$  at  $\hat{r} = 0$ . (48)

System or order ( $\epsilon^1$ ) for velocity profile:

$$\hat{r}\frac{d^2\hat{w}_1}{d\hat{r}^2} + \frac{d\hat{w}_1}{d\hat{r}} = \frac{\sigma}{(1+M)} \left(\frac{d\hat{w}_0}{d\hat{r}}\right)^3 + 3r \left(\frac{d\hat{w}_0}{d\hat{r}}\right)^2 \frac{d^2\hat{w}_0}{d\hat{r}^2}, \quad (49)$$

$$\hat{w}_1 = 0$$
 at  $\hat{r} = 1$ ,  $\frac{d\hat{w}_1}{d\hat{r}} = 0$  at  $\hat{r} = 0$ . (50)

### System of order ( $\epsilon^0$ ) for temperature profile:

$$(1+R)\frac{\mathrm{d}^2\widehat{\theta}_0}{\mathrm{d}\widehat{r}^2} + \frac{1}{\widehat{r}}\frac{\mathrm{d}\widehat{\theta}_0}{\mathrm{d}\widehat{r}} = -\Gamma(1+M)\left(\frac{\mathrm{d}\widehat{w}_0}{\mathrm{d}\widehat{r}}\right)^2, \quad (51)$$

$$\hat{\theta}_0 = 0$$
 at  $\hat{r} = 1$ ,  $\frac{d\hat{\theta}_0}{d\hat{r}} = 0$  at  $\hat{r} = 0$ . (52)

### System or order ( $\epsilon^1$ ) for temperature profile:

$$(1+R)\frac{d^{2}\widehat{\theta}_{1}}{d\widehat{r}^{2}} + \frac{1}{\widehat{r}}\frac{d\widehat{\theta}_{1}}{d\widehat{r}}$$

$$= -2\Gamma(1+M)\left(\frac{d\widehat{w}_{0}}{d\widehat{r}}\right)\left(\frac{d\widehat{w}_{1}}{d\widehat{r}}\right)$$

$$+\Gamma\sigma\left(\frac{d\widehat{w}_{0}}{d\widehat{r}}\right)^{4} - N_{1}\widehat{\theta}_{0}, \qquad (53)$$

$$\hat{\theta}_1 = 0$$
 at  $\hat{r} = 1$ ,  $\frac{d\hat{\theta}_1}{d\hat{r}} = 0$  at  $\hat{r} = 0$ . (54)

By solving each order of  $\epsilon$ , we have the following results for velocity profile:

$$\widehat{w}_0 = \gamma_0 \left( 1 - \widehat{r}^2 \right). \tag{55}$$

$$\widehat{w}_1 = \gamma_1 \left( 1 - \widehat{r}^4 \right). \tag{56}$$

Results for temperature profile:

$$\widehat{\theta}_0 = \lambda_0 \left( 1 - \widehat{r}^4 \right). \tag{57}$$

$$\hat{\theta}_1 = \lambda_6 \sigma \left( 1 - \hat{r}^6 \right) + N_1 \left( \lambda_3 \hat{r}^2 + \lambda_4 \hat{r}^6 + \lambda_5 \right). \tag{58}$$

The final expressions for temperature and velocity are:

$$\hat{w} = \gamma_0 \left( 1 - \hat{r}^2 \right) + \gamma_1 \left( 1 - \hat{r}^4 \right), \tag{59}$$

$$\hat{\theta} = \lambda_0 \left( 1 - \hat{r}^4 \right) + \lambda_6 \Lambda \left( 1 - \hat{r}^6 \right)$$

$$+ \delta \left( \lambda_3 \hat{r}^2 + \lambda_4 \hat{r}^6 + \lambda_5 \right). \tag{60}$$

# - Reynolds Model

For the case of variable viscosity model i.e., Reynolds model, we will set the values of viscosity in term of temperature as:

$$\hat{\mu} = e^{-L\hat{\theta}} \Rightarrow \frac{\mathrm{d}\hat{\mu}}{\mathrm{d}\hat{r}} = -L \, e^{-L\hat{\theta}} \frac{\mathrm{d}\hat{\theta}}{\mathrm{d}\hat{r}}.$$
 (61)

In view of the above setting, the equation of motion and heat equation is defined by:

$$-L\widehat{r}e^{-L\widehat{\theta}}\frac{d\widehat{\theta}}{d\widehat{r}}\frac{d\widehat{w}}{d\widehat{r}} + e^{-L\widehat{\theta}}\left(\frac{d\widehat{w}}{d\widehat{r}} + \widehat{r}\frac{d^{2}\widehat{w}}{d\widehat{r}^{2}}\right)$$

$$+M\left(\frac{d\widehat{w}}{d\widehat{r}} + \widehat{r}\frac{d^{2}\widehat{w}}{d\widehat{r}^{2}}\right) - \Lambda\left(\frac{d\widehat{w}}{d\widehat{r}}\right)^{2}\left[\frac{d\widehat{w}}{d\widehat{r}} + 3\widehat{r}\frac{d^{2}\widehat{w}}{d\widehat{r}^{2}}\right]$$

$$= c\widehat{r}, \qquad (62)$$

$$(1+R)\frac{d^{2}\widehat{\theta}}{d\widehat{r}^{2}} + \frac{1}{\widehat{r}}\frac{d\widehat{\theta}}{d\widehat{r}} + \delta\widehat{\theta}$$

$$+\Gamma\left(\frac{d\widehat{w}}{d\widehat{r}}\right)^{2}\left[e^{-L\widehat{\theta}} + M - \Lambda\left(\frac{d\widehat{w}}{d\widehat{r}}\right)^{2}\right] = 0, \quad (63)$$

The perturbation expansions on momentum and energy equations for this case are as follows:

$$\hat{w} \cong \hat{w}_0 + \varepsilon \hat{w}_1, \ \hat{\theta} \cong \hat{\theta}_0 + \varepsilon \hat{\theta}_1,$$

$$\Lambda \cong \varepsilon \sigma, \ \delta = \varepsilon N_1, \ L = \varepsilon l_1.$$
(64)

### System of order ( $\epsilon^0$ ) for velocity profile:

$$\hat{r}\frac{\mathrm{d}^2\hat{w}_0}{\mathrm{d}\hat{r}^2} + \frac{\mathrm{d}\hat{w}_0}{\mathrm{d}\hat{r}} = \frac{c\hat{r}}{(1+M)},\tag{65}$$

$$\hat{w}_0 = 0$$
 at  $\hat{r} = 1$ ,  $\frac{d\hat{w}_0}{d\hat{r}} = 0$  at  $\hat{r} = 0$ . (66)

### System or order ( $\epsilon^1$ ) for velocity profile:

$$\widehat{r}(1+M)\frac{d^{2}\widehat{w}_{1}}{d\widehat{r}^{2}} + (1+M)\frac{d\widehat{w}_{1}}{d\widehat{r}} \\
= l_{1}\widehat{\theta}_{0}\left(\frac{d\widehat{w}_{0}}{d\widehat{r}}\right) + l_{1}\widehat{r}\left(\frac{d\widehat{w}_{0}}{d\widehat{r}}\right)\left(\frac{d\widehat{\theta}_{0}}{d\widehat{r}}\right) \\
+ l_{1}\widehat{r}\widehat{\theta}_{0}\left(\frac{d^{2}\widehat{w}_{0}}{d\widehat{r}^{2}}\right) \\
+ \sigma\left(\left(\frac{d\widehat{w}_{0}}{d\widehat{r}}\right)^{3} + 3\widehat{r}\left(\frac{d\widehat{w}_{0}}{d\widehat{r}}\right)^{2}\frac{d^{2}\widehat{w}_{0}}{d\widehat{r}^{2}}\right) \tag{67}$$

$$\hat{w}_1 = 0$$
 at  $\hat{r} = 1$ , 
$$\frac{d\hat{w}_1}{d\hat{r}} = 0 \quad at \quad \hat{r} = 0. \tag{68}$$

## System or order $(\epsilon^0)$ for temperature profile:

$$(1+R)\frac{d^2\hat{\theta}_0}{d\hat{r}^2} + \frac{1}{r}\frac{d\hat{\theta}_0}{d\hat{r}} = -\Gamma(1+M)\left(\frac{d\hat{w}_0}{d\hat{r}}\right)^2, \quad (69) \quad - \text{ Vogel's Model}$$

$$\hat{\theta}_0 = 0$$
 at  $\hat{r} = 1$ ,  $\frac{d\hat{\theta}_0}{d\hat{r}} = 0$  at  $\hat{r} = 0$ . (70)

### System or order ( $\epsilon^1$ ) for temperature profile:

$$(1+R)\frac{d^{2}\widehat{\theta}_{1}}{d\widehat{r}^{2}} + \frac{1}{r}\left(\frac{d\widehat{\theta}_{1}}{d\widehat{r}}\right)$$

$$= -2\Gamma(1+M)\left(\frac{d\widehat{w}_{0}}{d\widehat{r}}\right)\left(\frac{d\widehat{w}_{1}}{d\widehat{r}}\right) + \Gamma\sigma\left(\frac{d\widehat{w}_{0}}{d\widehat{r}}\right)^{4}$$

$$+ l_{1}\widehat{\theta}_{0}\Gamma\left(\frac{d\widehat{w}_{0}}{d\widehat{r}}\right)^{2} - N_{1}\widehat{\theta}_{0}$$

$$(71)$$

$$\hat{\theta}_1 = 0$$
 at  $\hat{r} = 1$ ,  $\frac{d\hat{\theta}_1}{d\hat{r}} = 0$  at  $\hat{r} = 0$ . (72)

By solving each order of  $\epsilon$ , we have the following results for velocity profile:

$$\widehat{w}_0 = \gamma_0 \left( 1 - \widehat{r}^2 \right). \tag{73}$$

$$\hat{w}_1 = \gamma_2 l_1 \left( 2 - 3 \hat{r}^2 + \hat{r}^6 \right) + \gamma_3 \sigma \left( 1 - \hat{r}^4 \right).$$
 (74)

Results for temperature profile are:

$$\widehat{\theta}_0 = \lambda_0 \left( 1 - \widehat{r}^4 \right). \tag{75}$$

$$\hat{\theta}_{1} = \lambda_{7} \sigma \left( -1 + \hat{r}^{6} \right) + N_{1} \left( \lambda_{8} + \lambda_{9} \hat{r}^{2} + \lambda_{10} \hat{r}^{6} \right) + l_{1} \left( \lambda_{11} + \lambda_{12} \hat{r}^{4} + \lambda_{13} \hat{r}^{8} \right).$$
 (76)

The final expression for temperature and velocity are:

$$\widehat{w} = \gamma_0 \left( 1 - \widehat{r}^2 \right) + \gamma_2 L \left( 2 - 3\widehat{r}^2 + \widehat{r}^6 \right)$$

$$+ \gamma_3 \Lambda \left( 1 - \widehat{r}^4 \right), \tag{77}$$

$$\widehat{\theta} = \lambda_0 \left( 1 - \widehat{r}^4 \right) + \lambda_7 \Lambda \left( -1 + \widehat{r}^6 \right)$$

$$+ \delta \left( \lambda_8 + \lambda_9 \widehat{r}^2 + \lambda_{10} \widehat{r}^6 \right)$$

$$+ L \left( \lambda_{11} + \lambda_{12} \widehat{r}^4 + \lambda_{13} \widehat{r}^8 \right). \tag{78}$$

For Vogel's model, we take the values of viscosity as

$$\widehat{\widehat{\mu}} = e^{\left(rac{A}{B+\widehat{\widehat{ heta}}}-\widehat{\widehat{ heta}}_{
m w}
ight)}$$
, or  $\widehat{\widehat{\mu}} = e^{\left(rac{A}{B}-\widehat{\widehat{ heta}}_{
m w}
ight)}\left(1-rac{A\widehat{\widehat{ heta}}}{B^2}
ight)$ , and

$$\frac{\mathrm{d}\widehat{\mu}}{\mathrm{d}\widehat{r}} = -e^{\left(\frac{A}{B} - \widehat{\theta}_{\mathrm{w}}\right)} \left(\frac{A}{B^2}\right) \frac{\mathrm{d}\widehat{\theta}}{\mathrm{d}\widehat{r}}.$$

With the help of the above substitution, we get the equation of motion and heat equation in the following form:

$$(1+R)\frac{d^{2}\widehat{\theta}}{d\widehat{r}^{2}} + \frac{1}{\widehat{r}}\frac{d\widehat{\theta}}{d\widehat{r}} + \delta\widehat{\theta}$$

$$+ \Gamma\left(\frac{d\widehat{w}}{d\widehat{r}}\right)^{2} \left(\frac{1}{a}\left(1 - \frac{A\widehat{\theta}}{B}\right) + M - \Lambda\left(\frac{d\widehat{w}}{d\widehat{r}}\right)^{2}\right)$$

$$= 0, \tag{79}$$

where 
$$\delta = \frac{c_1}{e^{\left(\frac{A}{B} - \widehat{\theta}_{w}\right)}}$$
 and  $a = \frac{1}{e^{\left(\frac{A}{B} - \widehat{\theta}_{w}\right)}}$ .

The perturbation expansions for this case are as

follows:

$$\hat{w} \cong \hat{w}_0 + \varepsilon \hat{w}_1, \quad \hat{\theta} \cong \varepsilon \hat{\theta}_0 + \varepsilon^2 \hat{\theta}_1,$$

$$\Lambda \cong \varepsilon \sigma, \quad \delta \cong \varepsilon N_1, \quad \Gamma = \varepsilon \gamma, \tag{80}$$

### System of order ( $\epsilon^0$ ) for velocity profile:

$$\widehat{r}\frac{\mathrm{d}^2\widehat{w}_0}{\mathrm{d}\widehat{r}^2} + \frac{\mathrm{d}\widehat{w}_0}{\mathrm{d}\widehat{r}} = \frac{\widehat{r}}{1 + aM},\tag{81}$$

$$\hat{w}_0 = 0$$
 at  $\hat{r} = 1$ ,  $\frac{d\hat{w}_0}{d\hat{r}} = 0$  at  $\hat{r} = 0$ . (82)

### System of order ( $\epsilon^0$ ) for temperature profile:

$$(1+R)\frac{\mathrm{d}^2\hat{\theta}_0}{\mathrm{d}\hat{r}^2} + \frac{1}{r}\frac{\mathrm{d}\hat{\theta}_0}{\mathrm{d}\hat{r}} = -\gamma \left(\frac{1}{a} + M\right) \left(\frac{\mathrm{d}\hat{w}_0}{\mathrm{d}\hat{r}}\right)^2, (83)$$

$$\hat{\theta}_0 = 0$$
 at  $\hat{r} = 1$ ,  $\frac{d\hat{\theta}_0}{d\hat{r}} = 0$  at  $\hat{r} = 0$ . (84)

System or order ( $\epsilon^1$ ) for velocity profile:

$$\widehat{r}(1+Ma)\frac{d^{2}\widehat{w}_{1}}{d\widehat{r}^{2}} + (1+Ma)\frac{d\widehat{w}_{1}}{d\widehat{r}}$$

$$= \frac{A}{B^{2}}\frac{d\widehat{w}_{0}}{d\widehat{r}}\left(\widehat{\theta}_{0} + \widehat{r}\frac{d\widehat{\theta}_{0}}{d\widehat{r}}\right) + \frac{A}{B^{2}}\widehat{r}\widehat{\theta}_{0}\frac{d^{2}\widehat{w}_{0}}{d\widehat{r}^{2}}$$

$$+ a\sigma\left(\left(\frac{d\widehat{w}_{0}}{d\widehat{r}}\right)^{3} + 3\widehat{r}\left(\frac{d\widehat{w}_{0}}{d\widehat{r}}\right)^{2}\frac{d^{2}\widehat{w}_{0}}{d\widehat{r}^{2}}\right), \quad (85)$$

$$\hat{w}_1 = 0$$
 at  $\hat{r} = 1$ ,  $\frac{d\hat{w}_1}{d\hat{r}} = 0$  at  $\hat{r} = 0$ . (86)

System or order ( $\epsilon^1$ ) for temperature profile:

$$(1+R)\frac{d^{2}\widehat{\theta}_{1}}{d\widehat{r}^{2}} + \frac{1}{\widehat{r}}\frac{d\widehat{\theta}_{1}}{d\widehat{r}}$$

$$= -N_{1}\widehat{\theta}_{0} + \frac{1}{aB^{2}}\left(A\theta_{0}\gamma\left(\frac{d\widehat{w}_{0}}{d\widehat{r}}\right)^{2}\right) + \gamma\sigma\left(\frac{d\widehat{w}_{0}}{d\widehat{r}}\right)^{4}$$

$$-2\gamma\frac{d\widehat{w}_{0}}{d\widehat{r}}\frac{d\widehat{w}_{1}}{d\widehat{r}}\left(\frac{1}{a} + M\right),$$
(87)

$$\hat{\theta}_1 = 0$$
 at  $\hat{r} = 1$ ,  $\frac{d\hat{\theta}_1}{d\hat{r}} = 0$  at  $\hat{r} = 0$ . (88)

By solving each order of  $\epsilon$ , we have the following results for velocity and temperature profiles:

$$\widehat{w}_0 = \gamma_4 \left( 1 - \widehat{r}^2 \right). \tag{89}$$

$$\widehat{\theta}_0 = \lambda_{14} \left( 1 - \widehat{r}^4 \right). \tag{90}$$

$$\widehat{w}_{1} = \gamma_{5} A \left( 2 - 3\widehat{r}^{2} + \widehat{r}^{6} \right) + \gamma_{6} \sigma \left( 1 - \widehat{r}^{4} \right). \tag{91}$$

$$\widehat{\theta}_{1} = \lambda_{15} \left( -4\widehat{r}^{4} + \widehat{r}^{8} \right) + \lambda_{16} \left( 4\widehat{r}^{4} - \widehat{r}^{8} \right)$$

$$+ \lambda_{17} \left( 14\widehat{r}^{4} - 3\widehat{r}^{8} \right) + \lambda_{18} \left( -14\widehat{r}^{4} + 3\widehat{r}^{8} \right)$$

$$+ \lambda_{19} + \sigma \lambda_{22} \left( 1 - \widehat{r}^{6} \right)$$

$$+ N_{1} \left( \lambda_{23} \widehat{r}^{2} + \lambda_{24} \widehat{r}^{6} + \lambda_{25} \right). \tag{92}$$

The final expression for temperature and velocity are as follows:

$$\hat{w} = \gamma_4 \left( 1 - \hat{r}^2 \right) + \gamma_5 A \left( 2 - 3 \hat{r}^2 + \hat{r}^6 \right)$$

$$+ \gamma_6 \Lambda \left( 1 - \hat{r}^4 \right), \qquad (93)$$

$$\hat{\theta} = \lambda_{14} \left( 1 - \hat{r}^4 \right) + \lambda_{15} \left( -4 \hat{r}^4 + \hat{r}^8 \right)$$

$$+ \lambda_{16} \left( 4 \hat{r}^4 - \hat{r}^8 \right) + \lambda_{17} \left( 14 \hat{r}^4 - 3 \hat{r}^8 \right)$$

$$+ \lambda_{18} \left( -14 \hat{r}^4 + 3 \hat{r}^8 \right) + \lambda_{19} + \Lambda \lambda_{22} \left( 1 - \hat{r}^6 \right)$$

$$+ \delta \left( \lambda_{23} \hat{r}^2 + \lambda_{24} \hat{r}^6 + \lambda_{25} \right). \qquad (94)$$

### **Numerical Method**

The perturbation solution is compared with the explicit finite difference approximated numerical solution. The discretisation of the given domain  $\hat{r} \in [0, 1]$  can be accomplished in following manners

$$\hat{r}_i = \hat{r}_1 + (j-1)h_1$$
, for  $j = 1, 2, 3, \dots, m$ , (95)

where  $h_1 = 1/(m-1)$ , and  $\hat{r}_1 = 0$ . For the description of stencils, we put  $\hat{y} \equiv \hat{y}(\hat{r})$ . The finite difference approximation of first and second order derivatives, (respectively) can be written as

$$\hat{y}'_{1} = \left[ -\frac{1}{h_{1}}, 0, \frac{1}{h_{1}} \right] \begin{bmatrix} \hat{y}_{i-1} \\ \hat{y}_{i} \\ \hat{y}_{i+1} \end{bmatrix} + O(h_{1}^{2}), \quad (96)$$

$$\hat{y}''_{1} = \left[ -\frac{1}{h_{1}^{2}}, \frac{-2}{h_{1}^{2}}, \frac{1}{h_{1}^{2}} \right] \begin{bmatrix} \hat{y}_{j-1} \\ \hat{y}_{j} \\ \hat{y}_{j+1} \end{bmatrix} + O(h_{1}^{2}), \quad (97)$$

where  $\hat{y}_i = \hat{y}(r_i), \hat{y}'_i = \hat{y}'(r_i), \hat{y}''_i = \hat{y}''(r_i)$ 2, 3, ..., m-1. The boundary conditions can be defined

$$\hat{y}'(\hat{r}_j) = 0,$$
  $\hat{y}(\hat{r}_m) = 0.$  (98)

Stencil for one-sided first-order derivative which is also second-order accurate is

$$\hat{y}'_{i} = \left[ -\frac{3}{(2h_{1})}, \frac{2}{h_{1}}, \frac{-1}{(2h_{1})} \right] \begin{bmatrix} \hat{y}_{1} \\ \hat{y}_{2} \\ \hat{y}_{3} \end{bmatrix} + O(h_{1}^{2}) . \tag{99}$$

The boundary condition at  $\hat{r}_1$  is given by

$$\frac{-3}{2h_1}\hat{y}_1 + \frac{2}{h_1}\hat{y}_2 - \frac{1}{2h_1}\hat{y}_3 = 0, \tag{100}$$

or

$$-3\hat{y}_1 + 4\hat{y}_2 - \hat{y}_3 = 0. \tag{101}$$

The applications of above finite difference formulas to (40) and (41) provide the non-linear system of equations. To find the solution the resultant system, Newton method [27-35] is used.

# 5 Comparison with Previous Study

Our explicit finite difference numerical code is validated with the solution of [2]. For this, we solved the direct

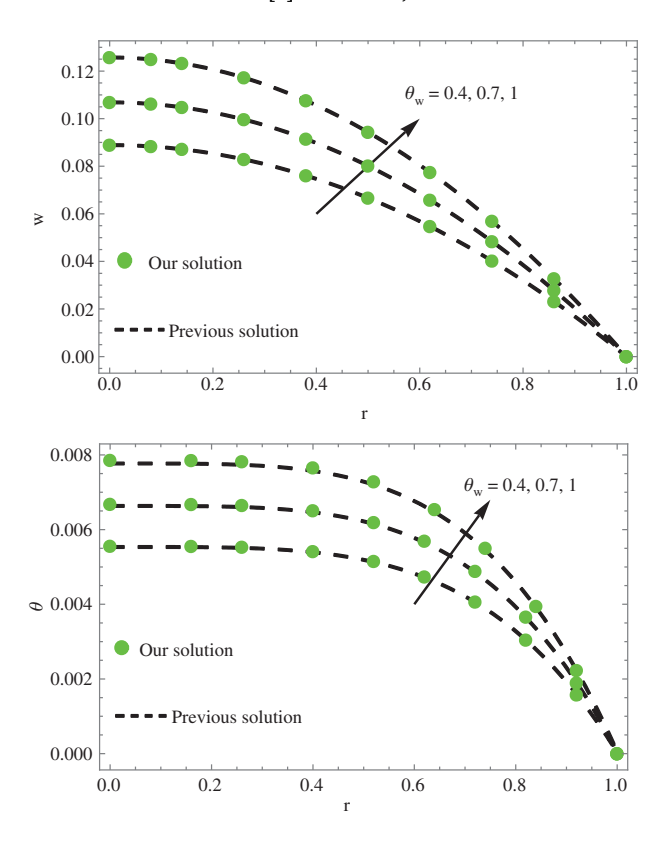


Figure 2: Velociy and temperature profiles for Vogel's viscosity model.

non-dimensional system of equations with boundary conditions of [2] with the help of our numerical code. The reported the solution of an EP fluid [2] under the account of constant and variable properties of viscosity in a pipe without the absence of thermal radiation and heat generation. The numerical results are presented for Vogel's viscosity model which are displayed in Figure 2 in term of velocity and temperature when  $R=\delta=0$ . From these figures, it can be seen that the solution of [2] and our solutions are in good agreement with each other.

### 6 Results and Discussion

The basic purpose of the current section is to explain the physical aspects of the emerging parameters on the distributions of velocity and temperature by considering the flow of EP fluid in a long circular pipe. Three famous models on the basis of viscosity property i.e., constant viscosity model, Reynolds model, and Vogel's model, respectively are discussed with the help of graphs.

To demonstrate the results of the given study, Figures 3–8 have been drawn. Figures 3–5 are related to the effects of different parameters on the velocity field, and Figures 6–8 display the effects of different parameters on the temperature field for all above-mentioned cases. These graphs exhibited the comparison of results of numerical solution and perturbation solution which are well agreed to each other. The results of the perturbation solution are represented by solid lines while the numerical solution is represented by a solid circle in each figure.

# **6.1 Effects of Dimensionless Parameters on Velocity Profile**

First, we discuss plots of velocity for the constant case. Figure 3a displays the effect of material parameter M on the velocity profile. We noticed that the velocity of the fluid decreases by increasing the value of material parameter M. The physical reason is that when we increase the values of M, the viscosity of the fluid also increases due to the direct relation between M and  $\mu(M=\frac{\mu}{X})$  as a result the fluid predicts the shear thickning effects, in this scenario the velocity of the fluid is decreasing [3]. Figure 3b shows the effect of parameter *c* on the velocity profile. The velocity of the fluid is increased by increasing magnitude of parameter c. When we increase the pressure of the fluid, the fluid taked more place in the vicinity of the pipe as a result the velocity increases. The influence of non-Newtonian parameter  $\Lambda$  on velocity distribution is shown in Figure 3c. It is noted that the velocity field predicts the increasing trend via

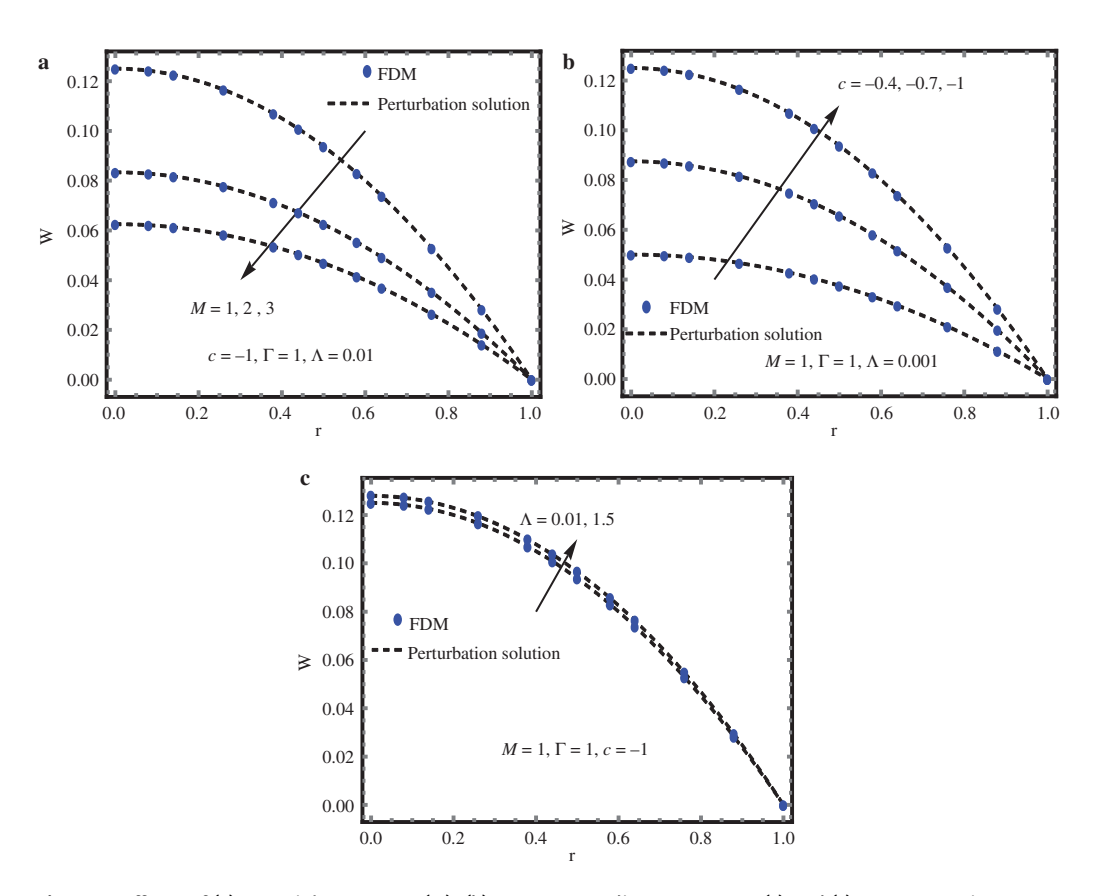


Figure 3: Effects of (a) Material parameter (M), (b) Pressure gradient parameter (c) and (c) non-Newtonian parameter ( $\Gamma$ ) on velocity profile.

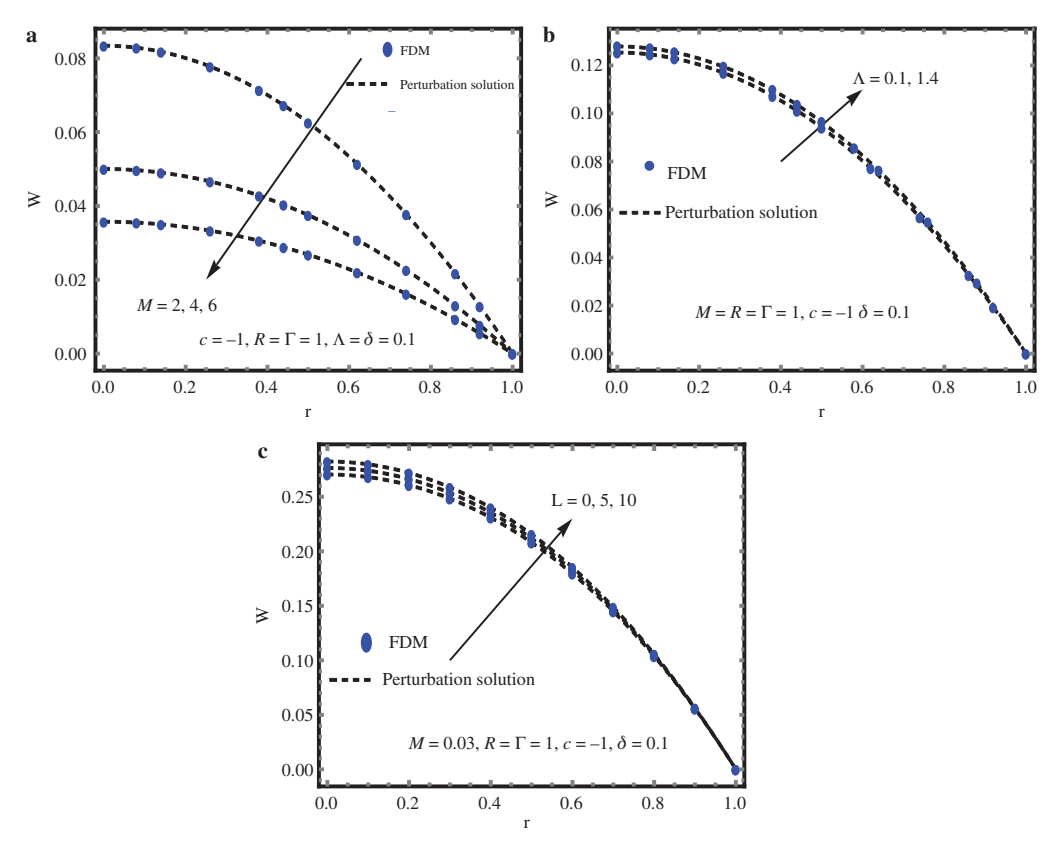


Figure 4: Effects of (a) Material parameter (M), (b) non-Newtonian parameter  $(\Gamma)$  and (c) Reynolds viscosity index (L) on velocity profile.

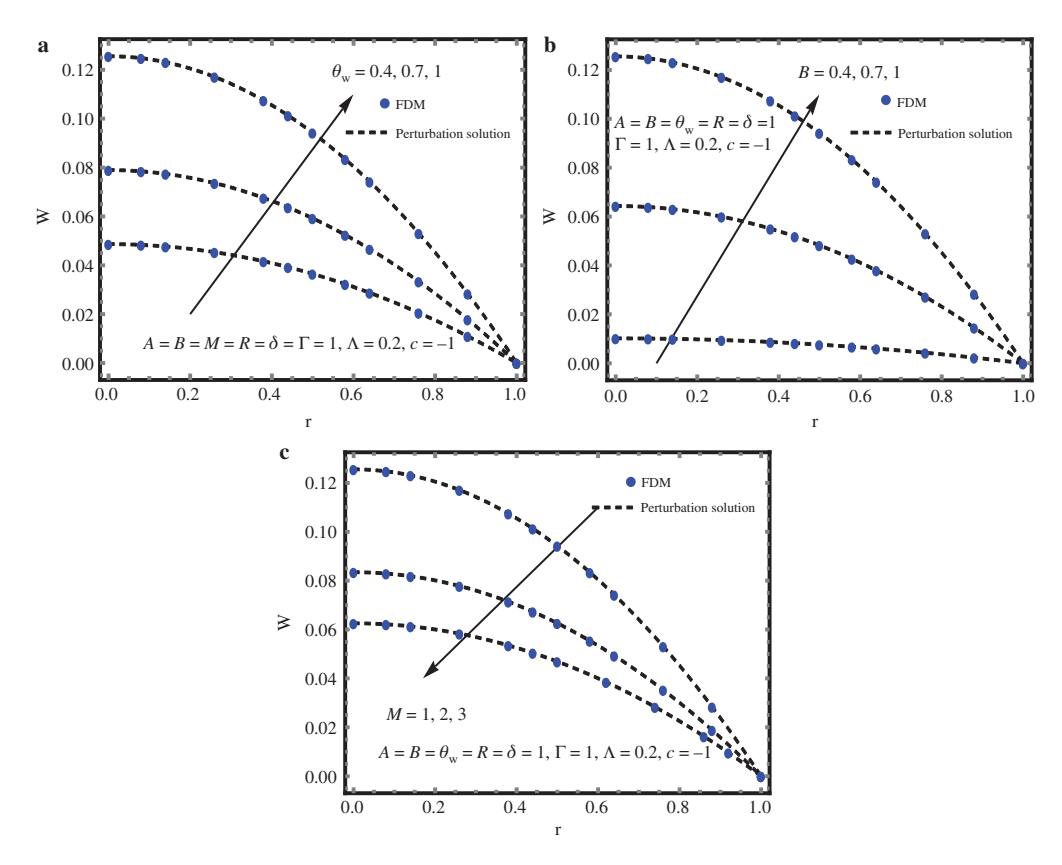
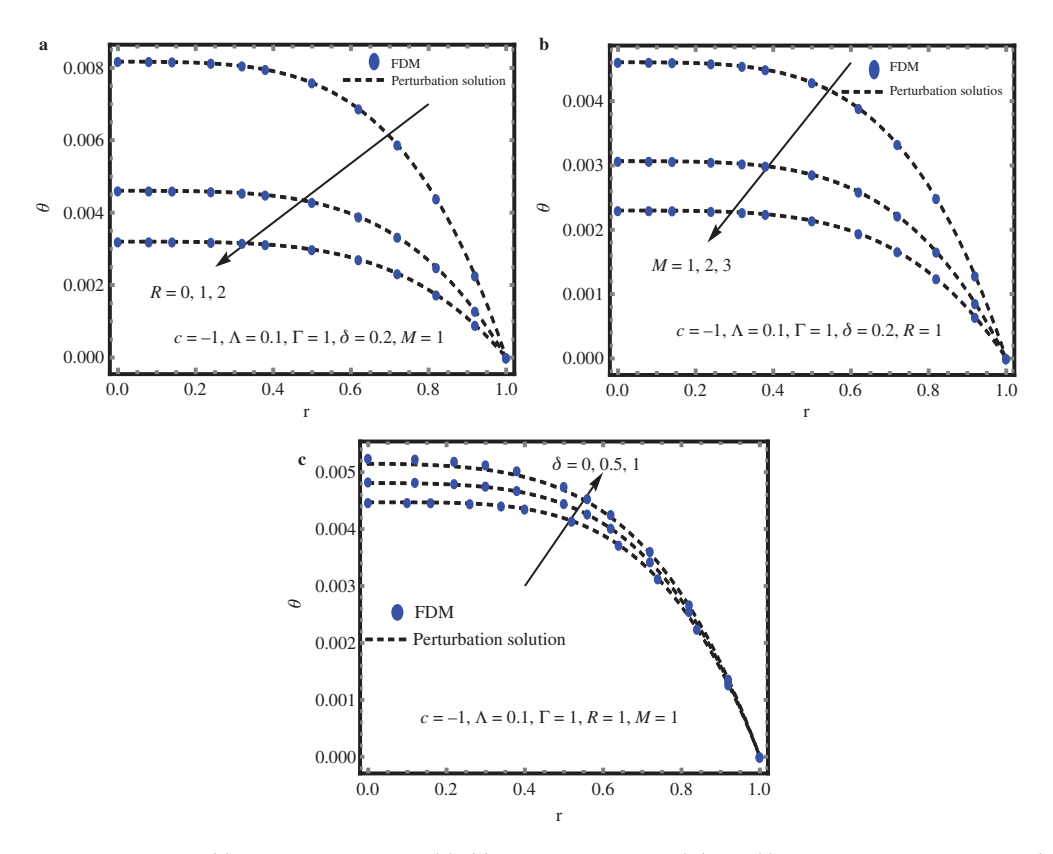


Figure 5: Effects of (a) Wall's temperature ( $\theta_w$ ), (b) Vogel's viscosity index and (c) Material parameter (M) on velocity profile.



**Figure 6:** Effects of (a) Radiation parameter (R), (b) Material parameter (M) and (c) Heat generation parameter ( $\delta$ ) on temperature profile.

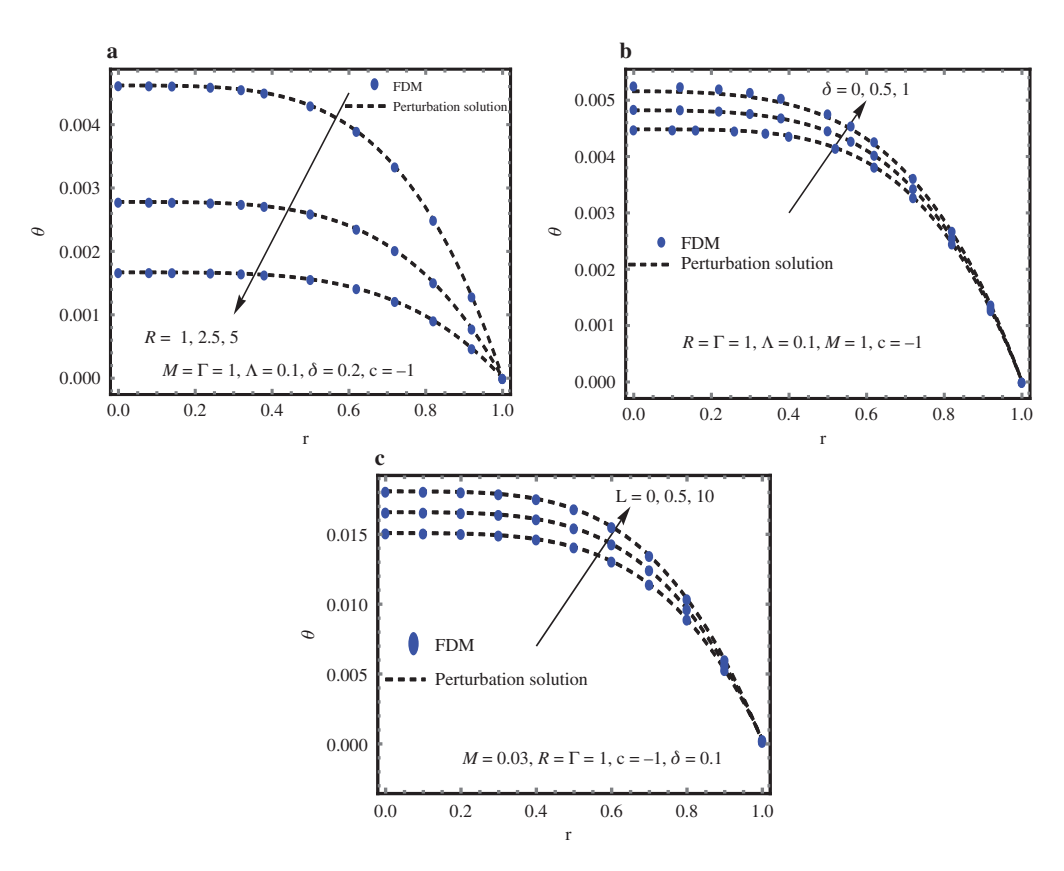
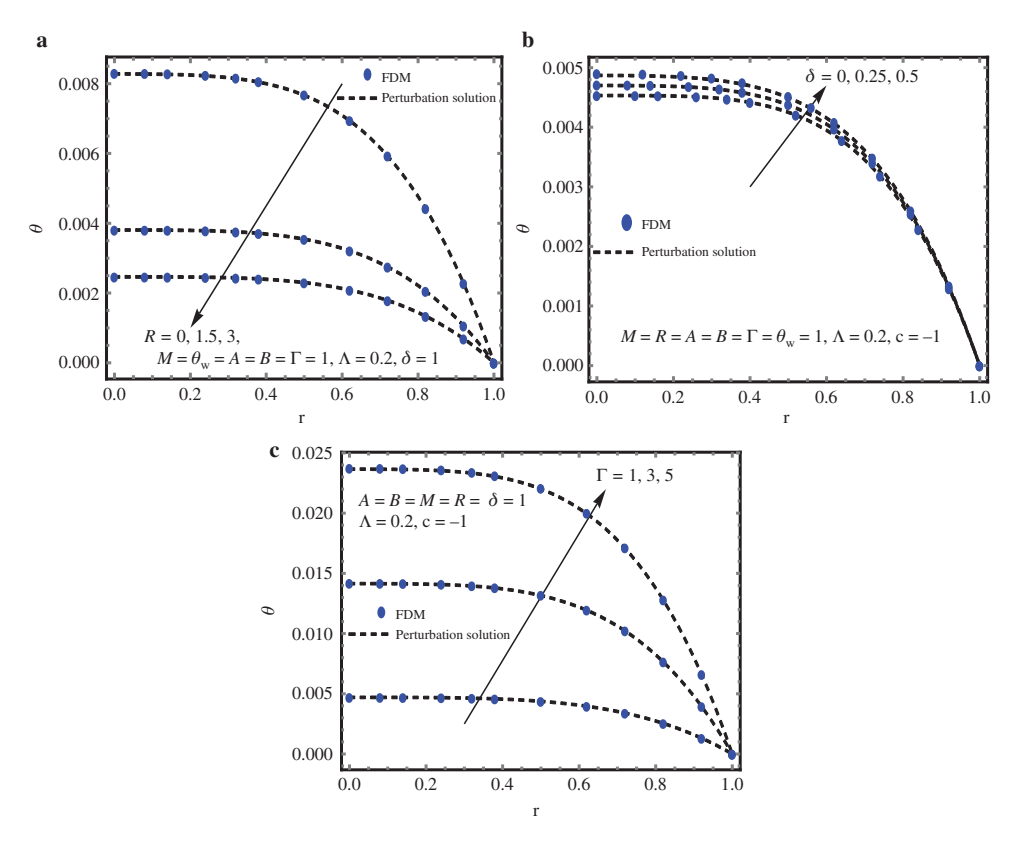


Figure 7: Effects of (a) Radiation parameter (R), (b) Heat generation parameter ( $\delta$ ) and (c) Reynolds viscosity index (L) on temperature profile.



**Figure 8:** Effects of (a) Radiation parameter (R), Heat generation parameter ( $\delta$ ) and (c) Viscous dissipation parameter ( $\Gamma$ ) on temperature profile.

 $\Lambda$  due to enhancement in the activation energy. Further, when  $\Lambda \to 0$ , the EP fluid behave as a Newtonian fluid. Next, we discuss plots of velocity for the case of Reynolds model. Figure 4a,b represents the effect of material parameter M and non-Newtoina fluid parameter  $\Lambda$  on the velocity profile. The velocity of the fluid is maximum at centreline of the pipe and minium near the walls of the pipe. The reported velocity profile shows the decreasing behaviour against the material parameter M. The effects of these both parameters on velocity profile is similar as we have explained in the previous case. The height of the velocity profile is minimum for the present case compared with the previous one. The influence of Reynolds viscosity index L on velocity is presented in Figure 4c. From this plot, it is observed, increase in the Reynolds viscosity index L enhances the velocity of the fluid. It is true, as increase in the Reynolds viscosity index L means diminishing absolute viscosity of the fluid and as a result the transfer of heat predicts the melting effects on the fluid which rises the fluid field. After this, the next three figures have been plotted for Vogel's viscosity model. The effects of temperature of the wall ( $\theta_{\rm w}$ ) on non-dimensionless velocity is shown in Figure 5. The velocity is increasing due to temperature of the wall. The reason is that when we increase the temperature of the boundary, the friction in the fluid is reduced as a results the velocity of the fluid is rise. The dimensionless velocity is enhance via Vogel's viscosity index (B) (see Fig. 5b) and reverse trend is observed via material parameter (*M*) as shown in Figure 5c.

# 6.2 Effects of Dimensionless Parameters on **Temperature Profile**

Here, Figures 6-8 are plotted to depict the effect of pertinent parameters on the temperature profile of all viscosity models. Figure 6a-c highlights the effect of radiation parameter (R), material parameter (M) and heat generation parameter ( $\delta$ ) for the case of uniform viscosity case. It is observed that the temperature is maxium at the

centre and decreases towards the walls of the pipe. The effects of radiation parameter have a decreasing trend on temperature (see Fig. 6a). Physically, when we increase the value of R, the absorption parameter diminish which means that less energy is absorbed by the fluid. The influence of material parameter on non-dimensional temperature is highlighted in Figure 6b and this figure reported the inverse relation of temperature and material parameter. It is scrutinised that the temperature increases with heat generation parameter. The physical reason is that the mechnasim of heat generation produces a hot layer within the fluid at moderate value of heat generation parameter as a result the fluid's temperature enhances via least temperature distribution in an infinite long pipe. The effects of radiation and heat generation parameters are displayed in Figures 7a,b and 8a,b. The physical phenomenon is observed for both paramters as we have discussed in the previous case of the viscosity model. The exclusion of radiation and heat generation is described for  $R \rightarrow 0$  and  $\delta \to 0$ , respectively. The behaviour of Reynolds viscosity index L is repoted in Figure 7c which demonstrate that the fluid's temperature slightly enhance with the enhancement of L. Physically, to increase the value of L leads to shear thinning effects as a result the temperature of the fluid increases. The effects of viscous dissipation parameter  $\Gamma$  on temperature distribution is highlighted in Figure 8c. From this figure, it is noted that increase in  $\Gamma$ , the dimensionless temperature profile increases due to rise in the kinetic energy within a moving fluid.

# 7 Error Magnitude

We compare the solutions obtained by the perturbation method and the explicit finite difference method. The absolute error in velocity and temperature distribution for the case of Reynolds viscosity model is listed in Table 1. From this table, it is noted that, the maximum absolute error in velocity and temperature is of the order of  $10^{-2}$ .

**Table 1:** Absolute error between analytical and numerical solutions for the case of Reynolds viscosity model M=1, c=-3, L=1,  $\Lambda=0.5$ ,  $\Gamma = 10$ .

R	δ	Perturbation Solution		Numerical Solution		Absolute Error	
		<b>W</b> max	$oldsymbol{ heta}_{\sf max}$	w <sub>max</sub>	$\boldsymbol{\theta}_{max}$	w <sub>E</sub>	$\theta_{\rm E}$
2	1	0.43652	0.37130	0.49977	0.41889	6.3 × 10 <sup>-2</sup>	$4.8 \times 10^{-2}$
3	1	0.42841	0.27183	0.47282	0.29605	$4.4 \times 10^{-2}$	$2.4  imes 10^{-2}$
4	1	0.42333	0.22923	0.45939	0.21403	$3.6  imes 10^{-2}$	$1.5  imes 10^{-2}$
5	0.4	0.41987	0.17051	0.45012	0.17899	$3  imes 10^{-2}$	$8.5 \times 10^{-3}$
5	0.7	0.41987	0.17344	0.45065	0.18293	$3 \times 10^{-2}$	$9.5 \times 10^{-3}$
5	1	0.41987	0.17637	0.45120	0.18702	$3.1 \times 10^{-2}$	$1.0 \times 10^{-2}$

This error increases with the increase in values of thermal radiation and heat generation parameters.

### Vogel's model

Figure 8

### 8 Conclusion

In this paper, we studied the combined effects of thermal radiation and heat generation in the one-dimensional flow of an EP fluid in a pipe. The dimensional governing momentum and energy equations are transformed into dimensionless form under the defined dimensionless quantities. In the present scenario, the viscosity is not only taken as a constant but it is also considered as a function of temperature namely Reynolds and Vogel's models. The highly non-linear boundary value problem is solved with the perturbation method as well as the finite difference method. The perturbation method is used to obtain the analytical expressions of velocity and temperature in each case. For the validation of our analytical solution, the eminent finite difference method is to pick and solve the direct dimensionless equations under the prescribed boundary conditions of each case of viscosity model.

The results of this study reveal the following effects:

- The velocity and temperature are decreasing functions of material parameter M.
- The influence of c and  $\Lambda$  are same in case of velocity function.
- The velocity is an increasing function of Vogel's model parameter B and  $\theta_{\rm w}$ .
- The temperature profile predcits the decreasing behaviour via material and radiation parameters and increment against heat generation parameter  $\delta$  and viscous dissipation parameter  $\Gamma$ .

### Solution benchmark [2]

Figure 2

### Plots for velocity:

### **Constant case:**

Figure 3

### Reynolds model

Figure 4

### Vogel's model

Figure 5

### **Constant case (Temperature graphs)**

Figure 6

### Reynolds model

Figure 7

### Nomenclature

R\* Radius of pipe M Material parameter Λ Non-Newtonian parameter Pressure gradient parameter Q Heat generation constant Bulk means fluid temperature  $\theta_m$ Viscosity of the fluid Cauchy's stress tensor X, YMaterial constants Rivlin-Ericksen tensor  $A_1$ Radiative heat flux  $H_R$ Heat absorption parameter Heat genration parameter Velocity components along z-direction Dimensionless radius Temperature of the fluid  $\hat{\theta}_{\mathrm{w}}$ Wall's temperature Thermal conductivity Reference velocity  $w_0$ Pressure of the fluid û Viscosity of the fluid Perturbation parameter Γ Viscous dissipation parameter В Α. Vogel's viscosity index L Reynolds viscosity index

# **Appendix**

Radiation parameter

R

$$\begin{split} \gamma_0 &= \frac{-c}{4(1+M)}, \quad \gamma_1 = \frac{2\sigma\gamma_0^3}{1+M}, \quad \gamma_2 = \frac{\gamma_0\lambda_0}{3(1+M)}, \\ \gamma_3 &= \frac{2\gamma_0^3}{1+M}, \quad \gamma_4 = \frac{-k}{4(1+aM)}, \\ \gamma_5 &= \frac{\gamma_4\lambda_{14}}{3B^2(1+aM)}, \quad \gamma_6 = \frac{2a\gamma_4^3}{1+aM}, \\ \lambda_1 &= -\frac{8\Gamma\gamma_0^4}{18+15R}, \quad \lambda_2 = \frac{8(1+M)\Gamma\gamma_0\gamma_1}{18+15R}, \\ \lambda_3 &= -\frac{\lambda_0}{4+2R}, \quad \lambda_4 = \frac{\lambda_0}{36+30R}, \\ \lambda_5 &= \frac{(8+7R)\lambda_0}{3(2+R)(6+5R)}, \quad \lambda_6 = \lambda_1 + \lambda_2, \\ \lambda_7 &= \frac{8\Gamma\gamma_0^4}{3(6+5R)}, \quad \lambda_8 = \frac{(8+7R)\lambda_0}{3(2+R)(6+5R)}, \\ \lambda_9 &= -\frac{\lambda_0}{4+2R}, \quad \lambda_{10} = \frac{\lambda_0}{36+30R}, \\ \lambda_{11} &= \frac{3(12+M(12+11R))\Gamma\gamma_0\gamma_2}{(4+3R)(8+7R)}, \end{split}$$

$$\lambda_{12} = -\frac{6(1+M)\Gamma\gamma_0\gamma_2}{4+3R}, \quad \lambda_{13} = \frac{3(1+M)\Gamma\gamma_0\gamma_2}{8+7R},$$

$$\lambda_{14} = \frac{(1+aM)\gamma \gamma_4^2}{a(4+3R)}, \quad \lambda_{15} = \frac{12A(1+aM)\gamma \gamma_4 \gamma_5}{a(4+3R)(8+7R)},$$

$$\lambda_{16} = \frac{2A \gamma \gamma_4^2 \lambda_{14}}{aB^2(4+3R)(8+7R)},$$

**DE GRUYTER** 

$$\lambda_{17} = \frac{AR\gamma \gamma_4^2 \lambda_{14}}{2aB^2(4+3R)(8+7R)},$$

$$\lambda_{18} = \frac{3A(1+aM)R\gamma\gamma_4\gamma_5}{a(4+3R)(8+7R)},$$

$$\lambda_{19} = \frac{A(12+11R)\gamma\gamma_4 \binom{6B^2(1+aM)}{\gamma_5-\gamma_4\lambda_{14}}}{2aB^2(4+3R)(8+7R)},$$

$$\lambda_{20} = \frac{8(1+aM)\gamma\gamma_4\gamma_6}{3a(6+5R)}, \quad \lambda_{21} = -\frac{8\gamma\sigma\gamma_4^4}{3(6+5R)},$$

$$\lambda_{22} = (\lambda_{20} + \lambda_{21}), \quad \lambda_{23} = -\frac{\lambda_{14}}{2(2+R)},$$

$$\lambda_{24} = \frac{\lambda_{14}}{6(6+5R)}, \quad \lambda_{25} = \frac{(8+7R)\lambda_{14}}{3(2+R)(6+5R)}.$$

# **References**

- [1] T. Hayat, Z. Igbal, M. Sajid, and K. Vajravelu, Int. Commun, Heat Mass Trans. 35, 1297 (2008).
- [2] N. Ali, F. Nazeer, and M. Nazeer, Z. Naturforsch. A73, 265 (2018).
- [3] A. A. Khan, F. Zaib, and A. Zaman, J. Braz. Soc. Mech. Sci. Eng. 39, 5027 (2017).
- [4] R. Ellahi, Appl. Math. Model 37, 1451 (2013).
- [5] A. T. Akinshilo and O. Olaye, J. King Saud Univ. Eng. Sci. 31, 271 (2017).
- [6] A. T. Akinbowale, Eng. Sci. Technol. Int. J. 20, 1602 (2017).
- [7] R. Ellahi and A. Raiz, Math. Comp. Model. 52, 1783 (2010).
- [8] Y. G. Aksoy and M. Pakdemirli, Trans. Porous Media 83, 375
- [9] R. Ellahi, T. Hayat, F. M. Mahomed, and S. Asghar, Nonlin. Anal. Real World Appl. 11, 139 (2010).

- [10] M. Farooq, M. T. Rahim, S. Islam, and A. M. Siddiqui, J. Assoc. Arab Univ. Basic Appl. Sci. 14, 9 (2013).
- [11] S. O. Alharbi, A. Dawar, Z. Shah, W. Khan, M. Idrees, E. Appl. Sci. 8, 2588 (2018).
- [12] T. Hayat, M. Awais, and S. Asghar, J. Egyptian Math. Soc. 21, 379 (2013).
- [13] M. Yurusov, Math. Comp. Appl. 9, 11 (2004).
- [14] T. Hayat, R. Naz, and S. Abbasbandy, Trans. Porous Media 87, 355 (2011).
- [15] M. Massoudi and I. Christie, Int. J. Non-Lin. Mech. 30, 687 (1995).
- [16] C. Huang, King Saud Univ. Eng. Sci. 30, 106 (2018).
- [17] T. Hayat, I. Ullah, A. Alsaedi, and M. Faroog, Results Phys. 7, 189 (2017).
- [18] T. Hayat and S. Nadeem, Results Phys. 7, 3910 (2017).
- [19] T. Hayat, S. Qayyum, S. A. Shehzad, and A. Alsaedi, Results Phys. 7, 562 (2017).
- [20] F. M. Abbasi, T. Hayat, B. Ahmad, and B. Chen, J. Cent. South Univ. 22, 2369 (2015).
- [21] G. M. Pavithra and B. J. Gireesha, J. Math. 2013, 583615 (2013).
- [22] V. D. Marcello, A. Cammi, and L. Luzzi, Chem. Eng. Sci. 65, 1301 (2010).
- [23] M. Nazeer, F. Ahmad, A. Saleem, M. Saeed, S. Naveed, et al., Z. Naturforsch. A 47, 961 (2019).
- [24] M. Nazeer, F. Ahmad, M. Saeed, A. Saleem, S. Khalid, et al., J. Braz. Soc. Mech. Sci. Eng. 41, 518 (2019).
- [25] N. Ali, M. Nazeer, T. Javed, and M. Razzag, Eur. Phys. J. Plus 2, 134 (2019).
- [26] M. Nazeer, N. Ali, and T. Javed, J. Porous Media 21, 953 (2018).
- [27] M. Nazeer, N. Ali, and T. Javed, Can. J. Phys. 96, 576 (2018).
- [28] N. Ali, M. Nazeer, T. Javed, and M. A. Siddiqui, Heat Trans. Res. 49, 457 (2018).
- [29] M. Nazeer, N. Ali, and T. Javed, Int. J. Numer. Methods Heat Fluid Flow 28, 10, 2404 (2018).
- [30] N. Ali, M. Nazeer, T. Javed, and F. Abbas, Meccanica 53, 3279 (2018).
- [31] M. Nazeer, N. Ali, T. Javed, and Z. Asghar, Eur. Phys. J. Plus 133, 423 (2018).
- [32] M. Nazeer, N. Ali, and T. Javed, Can. J. Phys. 97, 1 (2019).
- [33] M. Nazeer, N. Ali, T. Javed, and M. Razzaq, Int. J. Hydrog. Energy 44, 953 (2019).
- [34] M. Nazeer, N. Ali, T. Javed, and M. W. Nazir, Eur. Phys. J. Plus 134, 204 (2019).
- [35] W. Ali, M. Nazeer, and A. Zeeshan, 10th International Conference on Computational & Experimental Methods in Multiphase & Complex Flow, 21-23 May 2019, Lisbon, Portugal.